Multi-episode fluid boiling in the Shizishan copper-gold deposit at Tongling, Anhui Province: its bearing on ore formation

XIAO Xinjian (肖新建), GU Lianxing (顾连兴) & NI Pei (倪　培)

Department of Earth Sciences, State Key Laboratory of Mineral Deposit Research, Nanjing University, Nanjing 210093, China

Correspondence should be addressed to Gu Lianxing (email:lxgu@nju.edu.cn)

Received April 19, 2001

Abstract The Shizishan copper-gold deposit at Tongling, Anhui Province consists of two magmato-hydrothermal mineralization types: the crypto-explosive breccia type and the skarn type. At least four episodes of boiling occurred to the ore-forming fluids in this deposit. The first episode took place in accompany with the formation of the crypto-explosive breccias. The melt-fluid inclusions giving temperatures above 600℃ and salinities higher than 42% NaCl equiv represent a residual magma related to this episode. The second episode occurred during skarnization, giving fluid temperatures of 422℃—472℃, averaging 458℃, and salinities of 10.2%—45.1% NaCl equiv. The third episode corresponds to the main mineralization stage, i.e., the quartz-sulphide stage. Fluid temperatures of this episode vary in a range of 337℃—439℃ with an average of 390℃, and salinities in a range of 3%—30% NaCl equiv. The forth episode happened at the waning stage of mineralization, giving fluid temperatures below 350℃ with an average of 265℃ and salinities of 2.1%—40.4% NaCl equiv.

Keywords: copper-gold deposit, massive sulphide, fluid, boiling, Tongling.

The strata-bound copper-gold deposits in the Middle Carboniferous sequence of the Tongling district, Anhui Province are considered to represent submarine exhalative massive sulphide layers, which were transformed and overprinted by the Yanshanian (Mesozoic) magmas and their hydrothermal fluids[1—3]. Transformation and overprinting have not only added ore materials to the syn-sedimentary ore layers, but also produced new ore-bodies of the crypto-explosive breccia- and the skarn-types inside and at the contact zones of the Yanshanian granitoid bodies[1,4—7]. Primary discussions have been made by the present authors on the ore-forming fluids for the Middle Carboniferous sub-marine exhalative ores, but the characteristics of the Yanshanian overprinting fluids remain to be investigated. On the other hand, a large volume of literature has been yielded dealing with fluid boiling and its effect on mineralizations. Based on strong differences of fluid inclusions in pressure during homogenization, Rui Zongyao and his colleagues[8] proposed that one or more episodes of drastic pressure decrease could have occurred in some porphyry-type deposits and suggested that such pressure decrease was realized by fluid boiling. However, arguments are still rare about multi-episode boiling of ore-forming fluids. Based upon a case study on

fluid inclusions in the copper-gold ores of the crypto-explosive breccia and skarn types from the Shizishan deposit, this paper aims at demonstrating the multi-episode boiling of the Yanshanian overprinting fluids and its effect on ore formation.

1 Ore geology

1.1 Geology of the mine area

As seen on the surface and revealed by drilling (fig. 1), the sedimentary sequence of the Shizishan mine area, ranging from the Upper Devonian Wutong Formation up to Lower Triassic Tashan Formation, is characterized by marine clastics and carbonates. Intrusive rocks are dominated by diorite, quartz-diorite and quartz-monzodiorite. The Shizishan copper-gold deposit consists of the Eastern Shizishan and the Western Shizishan mines. The ores of the Western Shizishan mine belong to the skarn-type and occur at the contact zone of the quartz-monzodiorite body with Triassic limestone[9]. The ores of the Eastern Shizishan mine are controlled dominantly by a crypto-explosive breccia pipe in the quartz-monzodiorite. The funnel-shaped breccia pipe has a diameter of 150 m across its upper part, and extends down to a depth of more than 500 m (fig. 2).

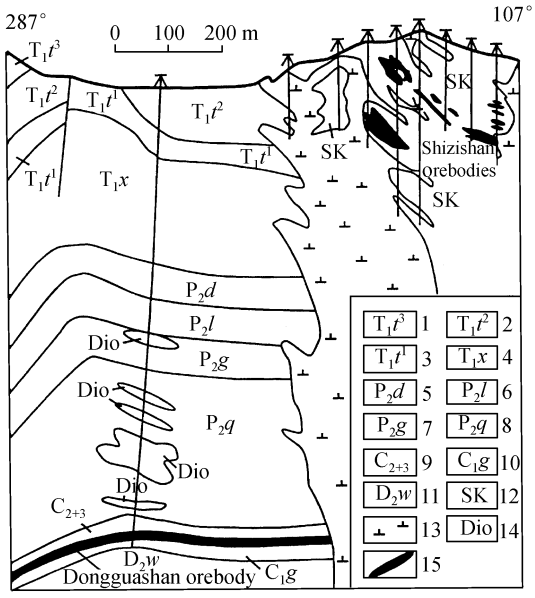

Fig. 1. Geology of Profile No. 42 of the Shizishan deposit (data from Geological Brigade No. 312, Bureau of Geology and Mineral Resources, Anhui Province, with modifications). 1, limestone of Upper Member of Tashan Fm.; 2, limestone of Middle Member of Tashan Fm.; 3, limestone and shale of Lower Member of Tashan Fm.; 4, Xiaoliangting Fm.; 5, siliceous limestone of Dalong Fm.; 6, sandstone of Longtan Fm.; 7, siliceous layer of Gufeng Fm.; 8, limestone of Qixia Fm.; 9, limestone of Huanglong and Chuanshan Fm.; 10, sandstone and shale of Gaolishan Fm.; 11, sandstone and shale of Wutong Fm.; 12, skarn; 13, quartz-monzodiorite; 14, diorite porphyry; 15, ore body.

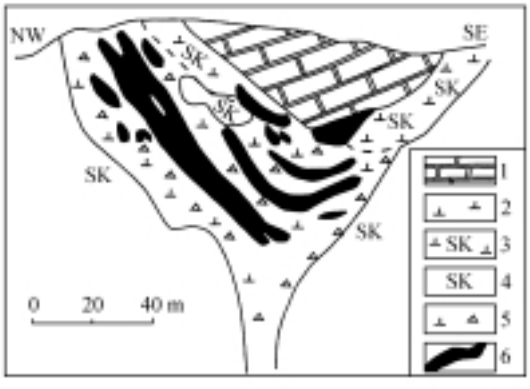

Fig. 2. Ore-bodies in the Eastern Shizishan breccia pipe (after ref. [10]). 1, marble; 2, quartz-monzodiorite; 3, skarnized quartz-monzodiorite; 4, massive skarn; 5, brecciated quartz-monzodiorite; 6, copper-gold ore.

The breccias, which are angular and chaotically arranged, are dominated in composition by quartz-monzodiorite and garnet skarn with minor marble and are cemented by garnet skarn. The pipe grades laterally into intensely skarnized quartz-monzodiorite and marble. The highest beds intruded by the Shizishan quartz-monzodiorite belong to the Triassic Tashan Formation. Based upon total thickness of the strata overlying the intrusion, it can be estimated that the apical part of the quartz-monzodiorite was emplaced at a depth of 700—1000 m and under a lithostatic pres-

sure of 18—26 MPa.

1.2 Ore types and mineralization stages

Based upon variations in compositions and textures, the copper-gold ores at Shizishan can be devided into the following types:

Crypto-explosive breccia-type ores occur inside the breccia pipe at Eastern Shizishan (fig. 2). The orebodies are lenticular or podiform. Gangue minerals are typified by andradite with very minor diopside, actinolite, quartz and carbonate. Sulphide minerals, which are dominated by chalcopyrite and pyrite, usually occur as disseminations, spots and patches. They can be found either in the matrix to the breccias together with gangue minerals, or as scattered replacement products inside the breccias.

Skarn-type ores occur in association with marble xenoliths lateral to the crypto-explosive breccia pipe at Eastern Shizishan, or at the contact zone between the intrusion and the surrounding marble at Western Shizishan. Skarn minerals in such a type of ores are dominated by diopside with only minor garnet. Chalcopyrite and pyrite are principal ore minerals in association with subordinate pyrrhotite, sphalerite, cubanite and molybdenite. Textures depicting sulphides replaced and penetrated by quartz and carbonates are commonly seen on hand specimen and under the microscope.

Quartz-sulphide-type ores are distributed mainly at the contact zone between the quartz-monzodiorite and marble at Western Shizishan, and can also be seen in the skarn pods lateral to the mineralized breccia pipe at Eastern Shizishan. Metal sulphides are dominated by pyrite, pyrrhotite and chalcopyrite with minor sphalerite. These minerals, in association with quartz and subordinate carbonates, often occur as replacive patches or veinlets in the skarn.

Quartz-carbonate-type ores mainly occur as sulphide-quartz-carbonate veins penetrating skarn and the breccia pipe. These veins are millimeters or centimeters in width, indicating their growth in open fractures. The sulphides, dominated by pyrite, chalcopyrite and sphalerite, often occur as spots or patches in a matrix of relatively coarser quartz and carbonates.

From the research on mineral paragenesis, the mineralization process of the Shizishan deposit are divided into four stages: the crypto-explosive breccia stage, the diopside skarn stage, the quartz-sulphide stage, and the sulphide-quartz-carbonate stage. The quartz-sulphide stage is the main stage for ore formation.

2 Ore-forming fluids

2.1 Experimental technique

Fluid inclusion measurements were made on LinKam THMS600 heating-freezing stages at State Key Laboratory of Mineral Deposit Research, Nanjing University with precisions better than ± 0.1℃ and ± 0.2℃ for freezing and homogenization temperatures, respectively. Combined freezing and heating determinations have performed on the same inclusions as long as possible.

To avoid overheating at temperatures approaching those for phase transition, the temperature would be lowered by 1℃ first, and then elevated slowly by an interval of 0.2℃. Attention was paid closely to the occurrence of phase transition. Repeated determinations were performed on the same inclusions in order to check possible leakage and get better precisions. The following formula was adopted for salinity calculations:

$$\text{Salinity} = 0.00 + 1.78X - 0.0442X^2 + 0.000557X^3,$$

where X represents absolute temperature of the freezing point[11]. Salinities of daughter-containing inclusions were obtained from temperatures at which the daughter minerals dissolved.

2.2 Fluid inclusion petrography

Melt-fluid inclusions as well as vapor-liquid two-phase and daughter-containing inclusions have been identified in the Shizishan deposit. Daughter minerals include halite, sylvine, calcite, etc. More than one daughters are found in some inclusions. Four main types of inclusions (table 1) are described below.

Table 1 Characteristics, temperatures and salinities of different-type fluid inclusions from Shizishan[a)]

Type	Host	Size /μm	Vap./liq. ratio (%)	T_{ice}/°C	Daughter	T_h/°C	Salinity (% NaCl equiv)	Sample No.	Boiling episode	Determ. No.
melt-fluid	garnet	10—44	15~80		+	＞600	42.0—56.2	M847, 846	1	7
	diopside	31	65		–	422		M848	2	1
vapor- rich	quartz	10—50	50~85	–19.4—–9.2	–	364—439 (408)	13.1—22.0 (17.5)	M841, 848 M839	3	11
	calcite	15—38	50~75	–9.4—–1.7	–	364—405 (393)	3.1—13.3 (6.7)	M848	3	5
	calcite					459—472 (461)	10.2—11.1 (10.6)	M841	2	5
	quartz	10—56	15~45	–2.7—–12.2	–	337—408 (376)	4.5—16.1 (10.2)	M839	3	21
liquid-rich daughter-free	calcite	13—31	30~40			394—410 (402)		M841	3	2
	quartz	5—63	10~25	–4.1—–7.2	–	196—336 (244)	6.6—10.7 (9.0)	M842, 840 M849, 847	4	6
	calcite	19—31	5~45	–1.2—–21.5 (–8.9)	–	148—333 (238)	2.1—23.4 (11.2)	M840, 842 M845, 848	4	12
	diopside	8—25	15~40		+	450—468 (460)	38.0—45.1 (40.4)	M843	2	10
liquid-rich daughter-bearing	quartz	19—31	25~30		+	427—428	29.0—30.0	M844	3	2
	calcite	19—53	10~20		+	244—334 (302)	31.4—40.4 (34.5)	M840	4	11
	quartz	6~25	15~25		+	269—294 (281)	25.2—32.9 (29.1)	M849	4	4

a) Numbers in brackets stand for average; +, daughter-bearing; –, daughter-free.

Melt-fluid inclusions (fig. 3(a)), which are composed of a melt phase and water solutions, are restricted to the garnet in the crypto-explosive breccias. They usually occur in isolation and measure 10—45 μm with irregular boundaries and sub-round bubbles. More than one daughters can be included, some of them being non-uniform in extinction. Vapor volume varies between 15% and 18%. This type of inclusions failed to be homogenized even at temperatures higher than 600℃.

Vapor-rich inclusions are composed of 50%—85% or more vapor with minor liquid phase (fig. 3(b)). They measure 10—50 μm across and occur dominantly in quartz and calcite inside

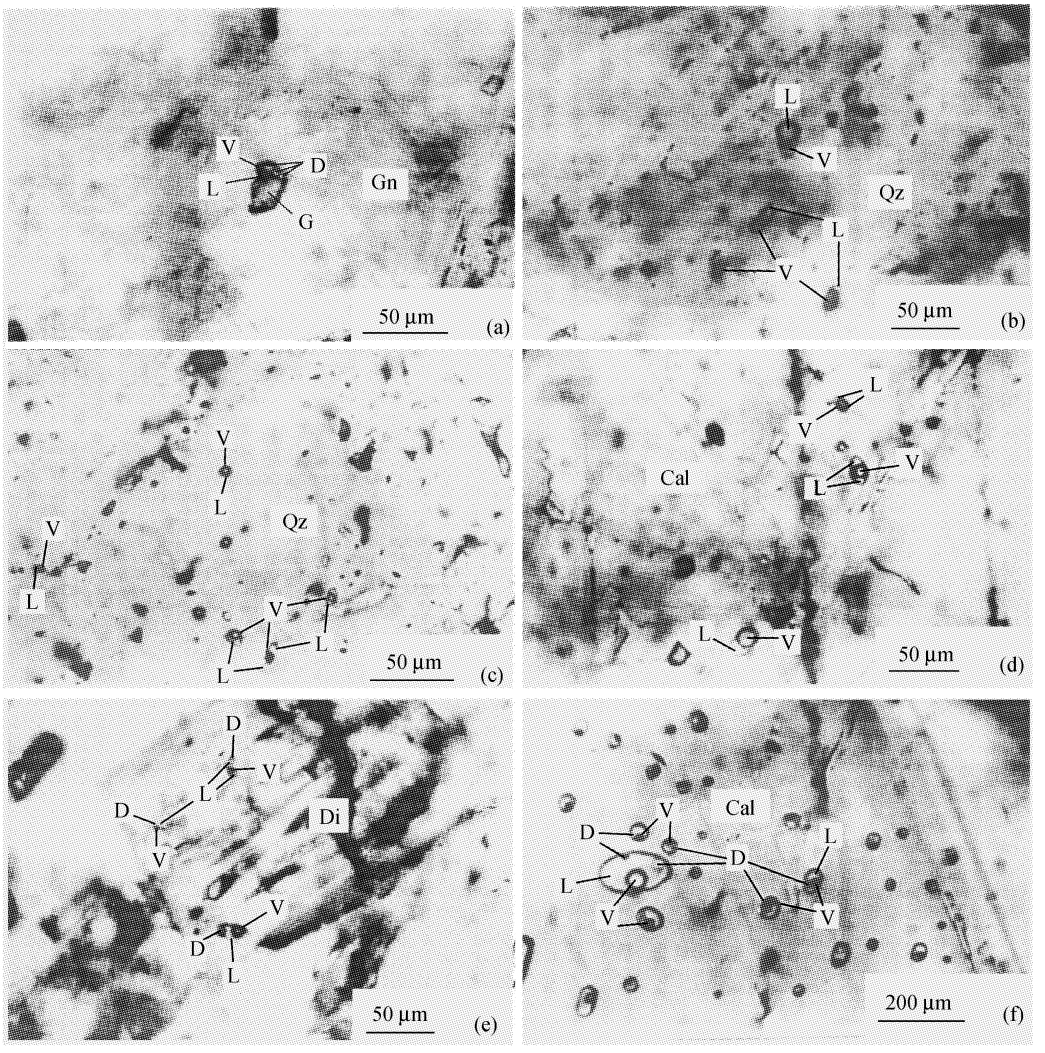

Fig. 3. Fluid inclusions of various types. Gn, garnet; Qz, quartz; Cal, calcite; Di, diopside; V, vapor phase; L, liquid phase; G, glass; D, daughter. (a) Melt-fluid inclusion in garnet including a vapor bubble with aqueous solution and glass. Sample M846, single nicol. (b) Vapor-rich inclusions (50%—85% vapor) coexisting with liquid-rich inclusions in quartz. Sample M858, single nicol. (c) Liquid-rich inclusions without daughter in quartz. Sample M839, single nicol. (d) Liquid-rich inclusions without daughter in a calcite patch. Sample M841, single nicol. (e) Liquid-rich and daughter-bearing inclusions in diopside. Sample M843, single nicol. (f) Liquid-rich and daughter-bearing inclusions coexisting with daughter-free inclusions. Sample M840, crossed nicols.

quartz-sulphide veins. There are also minor amounts of such a type of inclusions in diopside, actinolite and garnet, and in calcite and quartz patches inside the skarn-type ores. They often occur in clusters together with liquid-rich inclusions. Homogenization temperatures of them are normally higher than 350℃ with a maximum of 472℃.

Liquid-rich and daughter-free inclusions are characterized by two phases with aqueous liquid exceeding vapor in volume. They show light color with irregular boundaries and dimensions of 10—55 μm. Based on contrasting occurrences of host minerals, such a type of inclusions can be

distinguished into two groups. The first group refers to those included in quartz or patched calcite in quartz-sulphide veins and coexisting in clusters with vapor-rich inclusions (fig. 3(c), (d)). They are characterized by relatively higher homogenization temperatures of 350℃—420℃. The second group is hosted by quartz and calcite in quartz- calcite veins (fig. 3(e)). Inclusions of such a group often coexist with daughter-rich inclusions and normally give homogenization temperatures below 350℃.

Liquid-rich and daughter-bearing inclusions comprise vapor, liquid and daughter phases, and the vapor phase is usually less than 20%. There may be more than one grain of daughter minerals, which are dominantly halite and sylvite. These inclusions show irregular boundaries and have dimensions of 10—40 μm. Also, two groups are distinguished based on occurrences of their hosts. One group occurs in diopside, actinolite and quartz in skarn and coexists in clusters with vapor-rich inclusions and liquid-rich and daughter-free inclusions in quartz (fig. 3(e)). They give homogenization temperatures high up to 467.8℃. Another group is included in quartz and calcite in quartz-carbonate veins and coexists with liquid-rich and daughter-free inclusions (fig. 3(f)). Homogenization temperatures given by this type are usually lower than 350℃, but occasionally high up to 395℃.

2.3 Temperature and salinity

The data obtained are listed in table 1 and shown in fig. 4. The plots in fig. 4 do not include the samples on which either temperature or salinity determination is unsuccessful.

Garnet in the matrix of the crypto-explosive breccias in the intrusion is characterized by melt-fluid inclusions, which gave highest temperature and salinity values. All the temperature values of seven determinations exceeded the upper detection limit of the heating stage (600℃), and two of the inclusions gave salinities of 42.0 and 56.2% NaCl equiv, respectively. These two samples are plotted in area I of fig. 4.

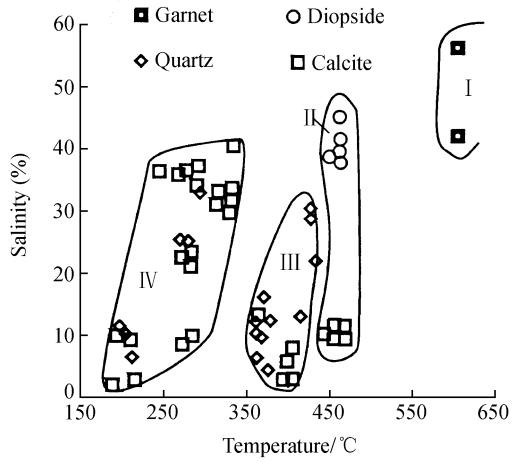

Fig. 4. Temperature-salinity relation of fluid inclusions for various stages of the Shizishan deposit.

Diopside in the skarn adjacent to the contact zone between the intrusive and marble contains both vapor-rich and daughter-bearing liquid-rich inclusions. Compared to those in garnet, inclusions in diopside gave lower temperatures and salinities, which are 422℃—467℃ and 38.0%—45.1% NaCl equiv, respectively. Calcite patches in the skarn are characterized by vapor-rich inclusions, which are homogenized at temperatures of 443℃—472℃, and have salinities of

10.2%—10.7% NaCl equiv. These two minerals show temperatures averaging 458 °C and are plotted in area Ⅱ of fig. 4.

Both vapor-rich and liquid-rich inclusions occur in clusters in calcite and quartz patches from the quartz-sulphide-type ores. Part of the liquid-rich inclusions contains one or more daughter grains. Inclusions in this type of ores gave homogenization temperatures of 337℃—439℃ with an average of 390℃, and salinities varying in a range of 3.0%—30.0% NaCl equiv, and are plotted in area Ⅲ of fig. 4.

Vapor-rich and liquid-rich inclusions coexist ubiquitously in late-stage quartz-carbonate veins. They yielded homogenization temperatures of 148℃—335.8℃ with an average of 265℃, and salinities in a range of 2.1%—40.4% NaCl equiv, and are plotted in area Ⅳ of fig. 4.

Calculations based on temperature and salinity of each stage and the equation of Souriaajan[12] yielded fluid pressures of ＞60, 50, 30 and 23 MPa for the crypto-explosive breccia, skarn, quartz-sulphide and quartz-calcite stages, respectively.

Based upon above-mentioned features in inclusion assemblages, temperatures and salinities and combined with geological relations, it can be suggested that the mineralizing fluids for the Shizishan deposit have undergone four episodes of fluid boiling. The first episode took place during the formation of crypto-explosive breccias. At temperatures exceeding 600℃, boiling of this episode produced the extremely high salinities of inclusion fluids in garnet. The second episode occurred in accompany with skarnization, resulting in the coexistence of diopside-hosted vapor-rich and daughter-bearing liquid-rich inclusions, both being homogenized at similar temperatures. The third and forth episodes correspond to the quartz-sulphide and quartz-carbonate mineralization stages. The clustered coexistence of vapor-rich low-salinity inclusions with liquid-rich high-salinity inclusions in quartz and calcite and the approximately equivalent homogenization temperatures of all these inclusions, demonstrate that boiling did occur at these two stages.

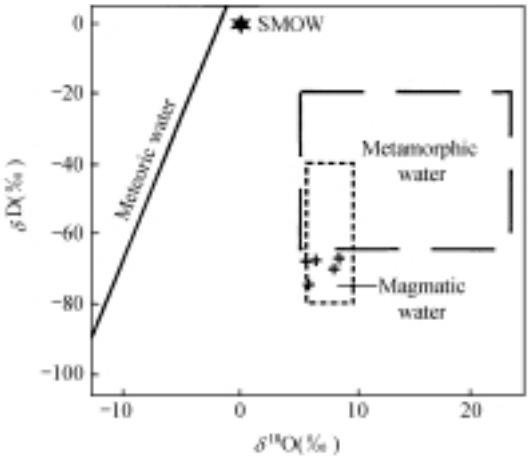

Fig. 5. δ^{18}O-δD plots of inclusion water in quartz [13].

2.4 Oxygen and hydrogen isotopes of fluids

Quartz separates from quartz-sulphide veins were determined for oxygen, hydrogen and carbon isotopes on a mass spectrometer Mat 252 in State Key Laboratory of Mineral Deposit Research, Nanjing University with analysis precisions better than 0.02%. The formula for calculation is $\delta_x - \delta_y \approx A \cdot 10^6 \cdot T^{-2} + B$, where A = 3.38 and B =

–3.40[14]. Oxygen and hydrogen isotope values for 5 samples are plotted basically in the region for magmatic water (fig. 5), indicating that ore-forming fluids were derived overwhelmingly from magmatic water with negligible involvement of waters from other sources. The $\delta^{13}C$ values (table 2) close to 0 imply that sedimentary carbonate beds assimilated by the magma are the major source for carbon in the fluids.

Table 2 Hydrogen, oxygen and carbon isotope compositions of quartz and its inclusion fluids(‰)

Sample number		M944	M953	M949	M858	M946
Mineralization stage		quartz-sulphide stage			quartz-carbonate stage	
Determ. value	T_h/℃	333	379	323	298	390
	$\delta^{18}O_{qz.SMOW}$	12.4	12.7	12.1	12.7	12.9
	$\delta D_{fluid.SMOW}$	–67.0	–69.5	–73.9	–67.3	–66.5
	$\delta^{13}C_{fluid.PDB}$	–2.89	4.97	0.94	–0.68	–2.95
Calculations of $\delta^{18}O_{fluid,\ SMOW}$		6.6	8.6	8.2	6.0	5.8

3 Discussion and conclusions

As mentioned in the foregoing sections, temperatures and salinities of ore-forming fluids in the Shizishan deposit vary in a wide range. The crypto-explosive breccia stage is characterized by homogenization temperatures exceeding 600℃ and salinities high up to 56.2% NaCl equiv. A considerable amount of literature has shown that high-salinity fluids in porphyry- and skarn-type deposits represent evolved magmatic fluids[15—19]. The plots of oxygen and hydrogen isotope values of the fluids from Shizishan in the magmatic region indicate that ore-forming fluids there were also derived from the magma. The overpressure gathering of magmatic fluids below the cooled rind in the apical zone of an intrusive body could be the main mechanism for crypto-explosion[20,21]. Being originally high, the salinities of the residual fluids left aside during drastic pressure reduction and boiling induced by crypto-explosion [22—24] were further raised, resulting in the acceleration of fluid evolution and ore formation.

Andradite in the matrix of crypto-explosive breccias is featured by melt-fluid inclusions. Homogenization temperatures of all these inclusions are higher than the upper detection limit (600℃) of the heating stage, indicating that fluid temperatures during trapping were approaching, or had reached the solidus of a water-rich granite melt [25,26]. Therefore, the authors would like to advocate the opinion of previous authors that the host garnet to these inclusions was formed by direct crystallization from a residual magma[27—29].

In contrast to garnet in the crypto-explosive breccias, diopside in the diopside-dominant skarn at the contact zones between the intrusive rocks and the surrounding marble or their xenoliths does not have melt-fluid inclusions, but has inclusions of slightly lower temperatures and salinities. The temperatures range from 422℃ to 472℃ with an average of 458℃, and salinities vary between 10.2% and 45.1% NaCl equiv. These temperatures are significantly lower than magma temperatures, indicating that such a sort of skarn is not formed by direct crystallization of

magma, but by reaction of the marble with high temperature fluids. The coexistence of vapor-rich inclusions, although too small for freezing point determinations, with daughter-bearing liquid-rich inclusions in diopside grains, and the existence of vapor-rich inclusions in calcite patches in the same samples appear to suggest that boiling also occurred during skarnization.

There is a great volume of literature dealing with the effect of fluid boiling on metal precipitation[22,23,30]. Boiling of the third episode could have caused temperature decrease of ore-forming fluids, rapid escape of H_2S and CO_2, and concentration of the solutes, leading to the precipitation of quartz, carbonates and sulphides, and thus initiated the principal mineralization stage of the Shizishan deposit. As boiling products, a large amount of replacive patches as well as fissure-filling veins of quartz and sulphides are likely to indicate that the high temperature fluids at that moment still had relatively higher energy, and thereby had strong percolating and reaction abilities. Boiling of this episode could have been driven by pressure release due to the formation of large volume of free spaces during skarnization of the marble. It has been shown that the replacement of 1 mole calcite by 1 mole diopside would produce 3.88 cm^3 free space in the rock[31].

The above-mentioned fluid pressures of all stages indicate that the first three episodes of boiling were induced by overpressure of the fluids with respect to the lithostatic pressure. By contrast, fluid pressure of the quartz-carbonate stage has been decreased to the same level as the lithostatic pressure, yet boiling is possible as a consequence of tectonic pressure-reduction. The product of the forth-episode boiling is represented substantially by quartz-carbonate veins containing a bit of sulphide minerals. These veins, largely millimeters to centimeters in width, have sharp walls, indicating that the emplacement of them was controlled by dilatant cracks. These cracks are likely to have been generated by volume contraction during cooling of the intrusion or by late-stage regional tectonism. It is just the pressure release induced by these dilatant cracks that have driven the fourth episode of boiling. Furthermore, the presence of dilatant cracks would have facilitated the escape of the vapor phase from fluids, resulting in the absence of vapor-rich inclusions coexisting with liquid-rich inclusions in quartz and carbonates. As a consequence, these two minerals are prevailed by daughter-free and daughter-bearing liquid-rich inclusions, which represent low-median and high salinities respectively. Owing also to rapid escape of the vapor phase, salinities of residual fluids increased so drastically that some of them have surpassed those formed at the quartz-sulphide stage. Fluids of so high salinities are able to leach metals from pre-existing ores. Consequently, it is reasonable to suggest that part of the ore-forming materials in these veins were derived by leaching from the ores formed at earlier stages.

As a summary, hydrothermal fluids of the Shizishan deposit were derived essentially from the magma. Multi-episode boiling of these late-magmatic and post-magmatic fluids accelerated ore-forming processes, or caused directly the precipitation of ore-forming materials, and is hence of great significance to copper-gold mineralizations. It is just the overprinting of ore-materials from these fluids that have resulted in the coexistence of the middle Carboniferous massive sulphide layers with the Yanshanian crypto-explosive breccia-type and the skarn-type deposits in the

Tongling district.

Acknowledgements This work was supported by the National Natural Science Foundation of China (Grant Nos. 49773194, 49733120) and Ministry of Geology and Mineral Resources (Grant No. 9501102-04-01). Many thanks should be given to the colleagues of Geological Brigade No. 321 and Shizishan Mining Company for their kind help during the fieldwork. The authors are indebted to Academician Chang Yinfo and Prof. Hu Shouxi for their constructive instruction throughout the present research.

References

1. Xu Keqin, Zhu Jinchu, Origin of the sedimentary- (or volcanosedimentary-) hydrothermally overprinted iron-copper deposits in some fault depression belts in Southeast China, Fujian Geology (in Chinese), 1978, (4): 1—68.
2. Fu Shigu, Geology of the pyrite-type copper deposits in the Lower Yangtze belt, Journal of Nanjing University (Natural Sciences Edition, in Chinese with English abstract), 1980, (4) : 43—67.
3. Gu Lianxing, Xu Keqin, On the Mid-Carboniferous submarine massive sulphide deposits in the lower reaches of the Changjiang (Yangtze) River, Acta Geologica Sinica (in Chinese with English abstract), 1986, (2): 176—188.
4. Chang Yinfo, Liu Xiangpei, Wu Yanchang, The Copper-Iron Belt of the Lower and Middle Reaches of the Changjiang River (in Chinese with English abstract), Beijing: Geological Publishing House, 1991, 1—379.
5. Gu, L. X., Hu, W. X., He, J. X. et al., Geology and genesis of Upper Palaeozoic massive sulphide deposits of South China, Applied Earth Science, Section B, 1993, 102: 83—96.
6. Zhai, Y. S., Xiong, Y. L., Yao, S. Z., Metallogeny of copper and iron deposits in the Eastern Yangtse Craton, east-central China, Ore Geology Reviews, 1996, 11: 229—248.
7. Gu, L. X., Hu, W. X., He, J. X. et al., Regional variations in ore composition and fluid features of massive sulphide deposits in South China: Implications for genetic modeling, Episodes, 2000, 23(2): 110—118.
8. Rui Zongyao, Huang Chongke, Qi Guoming, Porphyry Copper (Molybdenum) Deposits in China (in Chinese), Beijing: Geological Publishing House, 1984, 1—350.
9. Zhao Bing, Skarn-Type Deposits in China (in Chinese), Beijing: Science Press, 1989, 19—72.
10. Huang Xuchen, Chu Guozheng, Multistory metallogenic model of the Shizishan orefield in Tongling, Anhui Province, Mineral Deposits (in Chinese with English abstract), 1993, 12(3): 221—230.
11. Bodnar, B. J., Revised equation and table for determining the freezing point depression of H_2O-NaCl solutions, Geochemica et Cosmochemica Acta, 1993, 57: 683—684.
12. Souriaajan, S., Kennedy, G. C., The system H_2O-NaCl at elevated temperatures, Am. J. Sci., 1962, 260: 115—141.
13. Clayton, J. R., O'Neil, M. T., Oxygen isotope exchange between quartz and water, J. Geophys. Res., 1972, 77: 3057—3067.
14. Taylor, H. P., Oxygen and hydrogen isotope relationships, in Geochemistry of Hydrothermal Ore Deposits (ed. Barnes, H. L.), 2nd edition, New York: Wiley, 1979, 236—277.
15. Ahmad, S. N., Rose, A. W., Fluid inclusions in porphyry and skarn ores at Santa Rita, New Mexico, Econ. Geol., 1980, 75: 229—250.
16. Quan, R. A., Cloke, P. L., Kesler, S. E., Chemical analyses of halite trend inclusions from the granite porphyry copper deposit, British Columbia. Econ. Geol., 1987, 82: 1912—1930.
17. Roedder, E., Fluid inclusion evidence for immiscibility in magmatic differentiation, Geochim. et Cosmochim. Acta, 1992, 56: 5—20.
18. Xu, Z. W., Qiu, J. S., Ren, Q. J. et al., Geological and geochemical characteristics and genesis of the Shaxi porphyry copper (gold) deposits, Anhui Province, Acta Geologica Sinica, 1999, 73(1): 8—17.
19. Lu, H. Z., High temperature, salinity and highly concentrated ore metal fluids: an example from Grasberg Cu-Au porphyry deposit, Acta Petrologica Sinica, 2000, 16(4): 465—472.
20. Norton, D. L., Cathles, L. M., Breccia pipes——products of exsolved vapor from magmas, Econ. Geol., 1973, 68: 540—546.
21. Burnham, C. W., Magmas and hydrothermal fluids, in Geochemistry of Hydrothermal Ore Deposits (ed. Barnes, H. L.), third edition, New York: John Wiley & Sons, 1997, 63—124.

22. Drummond, S. E., Ohmoto, H., Chemical evolution and mineral deposition in boiling hydrothermal systems, Econ. Geol., 1985, 80: 126—147.
23. Khin, Z., Gemmell, J. B., Large, R. R. et al., Evolution and source of ore fluids in the stringer system, Hellyer VHMS deposit, Tasmania, Australia: evidence from fluid inclusion microthermometry and geochemistry, Ore Geology Reviews, 1996, 10: 251—278.
24. Zhu, Y. F., Zeng, Y. S., Ai, Y. F., Experimental evidence for a relationship between liquid immiscibility and ore-formation in felsic magmas, Applied Geochemistry, 1996, 11: 481—487.
25. Tuttle, O. F., Bowen, N. L., Origin of granite in the light of experimental studies in the system $NaAlSi_3O_8$-$KAlSi_3O_8$-SiO_2-H_2O, Geol. Soc. Amer. Mem., 1958, 74: 1—153.
26. Johannes, W., Holtz, F., Petrogenesis and experimental petrology of granitic rocks, Berlin: Springer, 1996, 1—335.
27. Wu Yanchang, On magmatic skarn——A new type of skarn, Geology of Anhui (in Chinese with English abstract), 1992, 2(1): 12—26.
28. Zhao Bing, Zhao Jinsong, Zhang Chongze et al., Experimental evidence for magmatogene Skran, Chinese Science Bulletin, 1993, 38(21): 1986—1989.
29. Tang Yongcheng, Wu Yanchang, Chu Guozheng et al., Geology of copper-gold polymetallic deposits in the along-Changjiang area of Anhui Province (in Chinese with English abstract), Beijing: Geological Publishing House, 1998, 1—351.
30. Yang Kaihui, Magmatic fluids and mineralization oberservations of subaerial volcanic-hydrothermal processes, black smokers on modern sea floor and melt inclusion studies, Earth Science Frontiers, 1998, 5(3): 7—38.
31. Seward, T. M., Barnes, H. L., Metal transport by hydrothermal ore fluids, in Geochemistry of Hydrothermal Ore Deposits (ed. Barnes, H. L.), third edition, New York: John Wiley & Sons, 1997, 435—486.